PERFORMANCE CHARACTERISTICS OF DETECTOR DEVICES USED IN LIDAR SYSTEM

B.ANUSHA SAMRAT[1], K.SAMBASIVARAO[2], Dr.K.RAGHUNATH[3]

M.Tech Student, Dept of ECE, Bapatla Engineering College, Bapatla, Andhra Pradesh, India[1]

Asst.Professor, Dept of ECE, Bapatla Engineering College, Bapatla, Andhra Pradesh, India[2]

Scientist / Engineer-SF, National Atmospheric Research Laboratory (NARL), Dept of Space, Gadanki, Tirupati, India[3]

Abstract: Lidar is an acronym for Light detection and Ranging. It is same as the principle of radar. Lidar is a powerful and versatile remote sensing technique in which a beam of light is used to make range resolved measurements and concentration of aerosol particles. Lidar applications need to deal with the detection of weak pulse signals, wide pass bands of receiving subsystem, and potentially intense sky background. The present work involves the processing of lidar signals under sky background for the prediction of APD/PMT (Avalanche Photodiode/Photo Multiplier Tube) detector performance and noise sources present in the atmosphere and in the electronics of the system reduces the performance of lidar. This process will mainly concentrate on the data collected from the signals under intense background conditions from a lidar situated at National Atmospheric Research Laboratory, Gadanki. This project deals with the performance of APD/PMT detectors under sky background. By normalizing all photo detector noises to quantum noise, to obtain quantitate expressions for degradation of signal to noise ratio, increasing threshold sensitivity, and decreasing lidar operation range. The lidar range taken at Ultra-Violet, Visible, Near Infrared region. Based on these observations the system performance can be predicted.

Keywords: Lidar, Photo detector, Avalanche Photodiode, Photo Multiplier Tube.

1. INTRODUCTION

Light detection and ranging (Lidar) is a technique in which a beam of light is used to make range-resolved remote sensing measurements. Lidar emits a beam of light and that interacts with the medium or particles under study and some of this light is backscattered towards the lidar receiver due to scattering of the light by the particles [5]. The backscattered light captured by the lidar receiver is used to determine the characteristics of the medium in which the beam propagated.

The Operation principle of Lidar is almost same as Radar; it is often sometimes called as laser Radar. The main difference between the Radar and Lidar is the wavelength of radiation it is used. Radar uses radio band wavelength and Lidar uses Light. A ground based lidar enables the measurement of the temperature profile in the stratosphere-mesosphere region (~30-80 km) with accuracy better than that can be achieved by other ground based rocket/satellite techniques. This also enables a systematic study of winds and waves in the middle atmosphere. Significantly, the altitude region of 30-80 km is beyond the capability of the Mesosphere-Stratosphere-Troposphere (MST) radar due to very weak backscattered echoes and for that reason, the two techniques are complementary to each other. Lidar is an atmospheric remote sensing tool. Vertical profiles of aerosol layers and

atmospheric temperatures derive from Lidar data [1]. Lidar is one of the most influential remote sensing techniques to explore the middle atmosphere of the earth. Latest developments leading to the availability of vast potential of lidars for atmospheric studies by more powerful, relatively rugged and highly proficient solid state lasers and development in data acquisition techniques and in detector technology. Atmospheric Lidar mainly works on the interactions, absorption and scattering of the light beam with the particles of the atmosphere. Many atmospheric parameters may be measured depending on the design of the Lidar, which includes aerosol properties, cloud properties, temperature, wind velocity etc. Lidars are now being used extensively in different parts of the globe to study aerosols/clouds (Mie Scattering), atmospheric density and temperature (Rayleigh Scattering), metallic ion species (Resonance Scattering), minor constituents and trace gases (Differential absorption), composition (Raman Scattering) and winds (Doppler Lidar).

At National Atmospheric Research Laboratory (NARL), Gadanki (13.8ºN, 79.2ºE) near Tirupati, India, a lidar system is present in which the Lidar transmitter employs an Nd: YAG pulsed laser that is a solid-state class of laser source. The lidar studies over tropics are rather unclear,

although the atmospheric phenomena allied with this region are of significant importance.

2.SYSTEM CONFIGURATION

2.1 Transmitter sub-system:

The laser transmitter employs a PL9050 model Nd:YAG pulsed laser (solid state laser) from Continuum, USA.
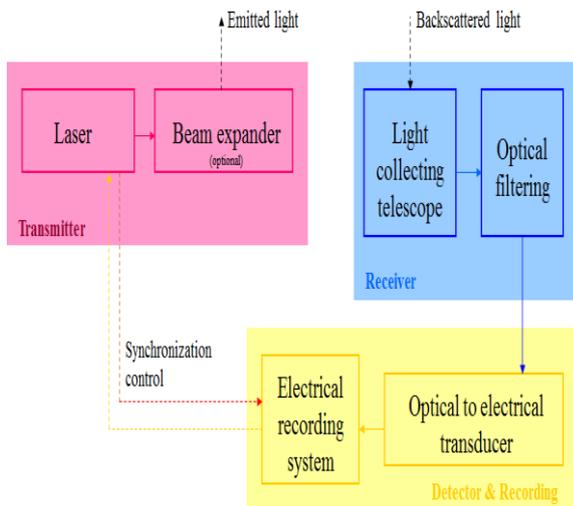

Figure 2.1: Generic block diagram of lidar

The laser head is of modular design incorporating a rod, flash-lamp(s) and coupling medium. The flash lamps are surrounded by a diffuser (magnetic oxide), which results in a high pumping efficiency that minimizes thermal loading and reduces power consumption. In which it consists of an Nd:YAG laser source of 532nm wave length operating in a pulsed mode of 50Hz pulse repetition rate, in which it delivers an average output power of 30W.

2.2 Receiver sub-system:

Two telescopes receive the backscattered signal, the independent receivers are used to receive Rayleigh and Mie backscattered signals.

The Rayleigh receiver operates in the range of 30 to 80 km, used for collecting the backscattered light from the air molecules, it has two channels named as R-Channel and U-Channel in which a Newtonian type telescope is using as receiver. Whereas Mie receiver operates in the range of 4 to 40 km, used for collecting the backscattered light from particles such as aerosols, Hydrometeors etc, it also has two channels named as P-Channel and S-Channel in which a vertical Schmidt-Cass grain type telescope is using as receiver. The received signal is usually processed to filtering, it significantly reduces background.

2.3 Detector and Recording sub-system:

After filtering it is focused to an optical detector PMT (photo multiplier tube) that converts optical signal to electrical signal. The output of PMT is in the form of current pulses; it can be recorded electronically the electrical pulses due to individual photons are counted the output of the PMT is filtered using a discriminator to remove a substantial number of the dark counts in which a threshold level is settled between the amplitude of signal count and dark count. Dark counts arise because of the thermal emission of electrons inside the PMT. The average dark count gain will be less than the averaged photon-induced gain, i.e., the average dark-count pulse amplitude is less than the average photon-induced pulse amplitude. This allows the use of a discriminator that selectively passes pulses that have amplitude greater than threshold level. Triggers are given to gating, +200 V. The counting of the electrical pulses is typically achieved using a Multichannel scalar (MCS).

3. APD/PMT DETECTORS

3.1 APD (Avalanche photodiodes)

Avalanche Photodiodes (APDs) are high sensitivity, high speed semi-conductor "light" sensors [3]. Compared to regular PIN construction photodiodes, APDs, have an internal region where electron multiplication occurs, by application of an external reverse voltage, and the resultant "gain" in the output signal means that low light levels can be measured at high speed. Incident photons create electron – hole pairs in the depletion layer of a silicon photodiode structure and these move towards the respective PN junctions at a speed of up to 105 meters per second, depending on the electric field strength. If the external bias increases this localized electric field to above about 105 V / cm then the carriers in the semi-conductor collide with atoms in the crystal lattice, and the resultant ionization creates more electron – hole pairs, some of which then go on to cause further ionization giving a resultant gain in the number of electron – holes generated for a single incident photon (See schematic below).
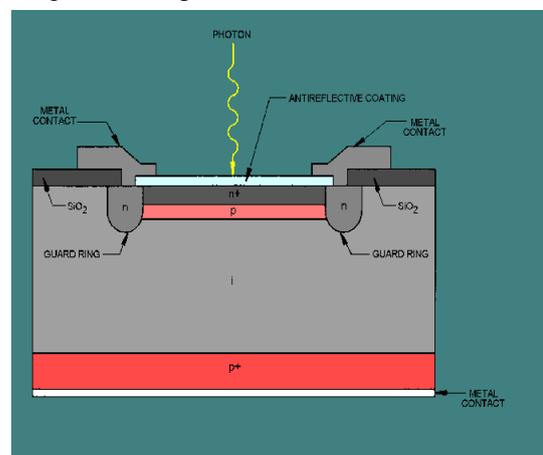

Figure 3.1: STRUCTURE OF APD

Most commonly available APDs are fabricated from silicon and employ a so called "reach through" structure where light is incident from the N-side of the silicon.

These devices show useful sensitivity in the 450 nm to 1000 nm wavelength range, such as the S6045 series from Hamamatsu Photonics. It is possible to fabricate devices where light is incident from the P-side, such as the S8664 series from Hamamatsu Photonics, and these then exhibit high sensitivity to UV – blue light and operate in the range from 200 nm to 800 nm. APD gain is typically in the range from x10 to x300 for most commercial devices, but there are APDs available from specialist manufacturers with gains of thousands. This then can give a significant advantage over regular PIN photodiodes for applications which are short of photons and where it is not possible to integrate these low signals.

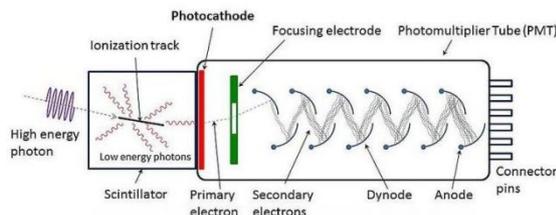3.2 PMT (Photomultiplier tube)

Figure 3.2: PMT (Photomultiplier tube)

Photomultipliers are constructed from a glass envelope with a high vacuum inside, which houses a photocathode, several dynodes, and an anode. Incident photons strike the photocathode material, which is present as a thin deposit on the entry window of the device, with electrons being produced as a consequence of the photoelectric effect. These electrons are directed by the focusing electrode toward the electron multiplier, where electrons are multiplied by the process of secondary emission.

The electron multiplier consists of a number of electrodes called dynodes. Each dynode is held at a more positive voltage, by ≈100 Volts, than the previous one. A primary electron leaves the photocathode with the energy of the incoming photon, or about 3 ev for "blue" photons, minus the work function of the photocathode. As a group of primary electrons, created by the arrival of a group of initial photons, moves toward the first dynode they are accelerated by the electric field. They each arrive with ≈100 ev kinetic energy imparted by the potential difference. Upon striking the first dynode, more low energy electrons are emitted, and these electrons in turn are accelerated toward the second dynode. The geometry of the dynode chain is such that a cascade occurs with an ever-increasing number of electrons being produced at each stage. For example, if at each stage an average of 4 new electrons are produced for each incoming electron, and if there are 12 dynode stages, then at the last stage one expects for each primary electron about $5^{12} \approx 10^8$ electrons. This large number of electrons reaching the last stage, called the anode, results in a sharp current pulse that is easily detectable, signaling the arrival of the photon at the photocathode about a nanosecond earlier.

There are two common photomultiplier orientations, the head-on or end-on (transmission mode) design, as shown above, where light enters the flat, circular top of the tube and passes the photocathode, and the side-on design (reflection mode), where light enters at a particular spot on the side of the tube, and impacts on an opaque photocathode. The side-on design is used, for instance, in the type 931, the first mass-produced pmt. Besides the different photocathode materials, performance is also affected by the transmission of the window material that the light passes through, and by the arrangement of the dynodes. A large number of photomultiplier models are available having various combinations of these, and other, design variables. Either of the manuals mentioned will provide the information needed to choose an appropriate design for a particular application.

4. INFLUENCE OF BACKGROUND ON SNR

The elastic lidars with moderate pulse energies, and for all Raman lidar applications, the important factor that limits the detection of weak signals in day time is the sky background. Lidar applications need to deal with the detection of weak pulse signals, wide pass bands of the receiving subsystem, and potentially intense sky background. Generalize the signal background analysis to all values of received echo signals, external backgrounds and internal noises, all sources, irrespective of their nature, are normalized to quantum noise which determines the maximum limit of SNR.

4.1   Mathematical Expressions

A. Variations of Background and Internal Noise Depending on the Receiver Pass Band

The conventional approach to analyze the relation between lidar echo signals, external backgrounds and internal noise has been discussed in the laser remote sensing and is based on the use of photo detectors. It requires taking into account a large number of specific component parameters for different lidar photo detectors. The signal to noise ratio is can be written as

$$\text{SNR}=\rho=\frac{I_s}{\sqrt{2q\Delta f[(I_s+I_b+I_d)F+I_L]+\left(\frac{4kT\Delta fF_A}{R_LM^2}\right)+\left(\frac{I_A^2}{M^2}\right)}} \quad (4.1)$$

To estimate the signal background analysis to all values of received echo signals, external backgrounds and internal noises, all sources , are normalized to the quantum noise which determines the maximum SNR it is used to estimate the excess noise factor in relation to the shot noise.

The signal to noise ratio at the output of a generalized system of photo detection is given as follows [2]

$$P=\frac{P_s}{\sqrt{\left(\frac{2hc\Delta fF}{\eta\lambda}\right)(P_s+P_b)+(NEP)^2\Delta f}} \quad (4.2)$$

Here, we are taken the three normalized parameters those are $\Psi_s = P_s/P_q, \Psi_b = P_b/P_q, \Psi_n = P_n/P_q$

Where, $P_s = \frac{A}{R^2 P_q}$

$P_b = B_\lambda A_r \Omega \Delta\lambda\varepsilon_0,$

$P_n = NEP.\Delta f^{1/2}$, $P_q = 2hcF\Delta f/\lambda\eta$ By using these equations we are solving the **FIG 5.1**.

B. Photo Detector Threshold Sensitivity Due to External Background

The influence of sky background is completely determined by U-parameter which can be considered as the factor of the excess noise caused by sky background. The fractional decrease of lidar sensitivity due to the background is equal to the u-parameter

$$U \equiv \frac{P_t}{P_{t0}} = \frac{\Psi_s^{min}}{\Psi_s^{min}(\Psi_b=0)} = \frac{1+\sqrt{1+\left(\frac{4}{\rho^2}\right)\Psi_n^2(1+(\Psi_b/\Psi_n^2))}}{1+\sqrt{1+(\frac{4}{\rho^2})\Psi_n^2}}$$

(4.3)
By using above equation to solve the **FIG 5.2** the noisy photo detectors are less sensitive to the external back ground influence.

C. Comparison Of Different Approximations Of The External Background Influence

The particular limiting expressions for the U-parameter which measures the decrease in S/N due to the increase noise components for the case ρ=1 are represented in **FIG 5.3**.

$$U \equiv \frac{P_t}{P_{t0}} = \frac{\Psi_s^{min}}{\Psi_s^{min}} = \frac{1+\sqrt{1+\left(\frac{4}{\rho^2}\right)\Psi_n^2(1+(\Psi_b/\Psi_n^2))}}{\frac{1}{2}\rho^2\left(1+\sqrt{1+\frac{4}{\rho^2}(\Psi_b+\Psi_n^2)}\right)}$$(4.4)

As one can see the approximation U1 leads to overestimation of the background impact, and the applicability of both curves U1 and U2 is limited by very low-noise photo detectors.

D. Reduction of Lidar Operating Range

Estimate the reduction of lidar operating range under sky background the lidar echo signal power Ps as

$$\Psi_s = \frac{Ps}{Pq} = \frac{A}{R2Pq}$$

where A is proportionality factor by neglecting for simplification the signal extinction in relatively transparent atmosphere and taking into account only its geometrical extinction that proportional to a range squared.

The ratio $r_b = U^{-1/2}$ (4.5)
The ratio r_b is in a form when it depends only on dimensionless powers of the background and internal noise levels are smaller from the above r_b, we got **FIG 5.4**.

E. Generalized Photo Detector Models

Lidar operates at near –UV, visible, and a near-IR spectral region which corresponds to the highest levels of sky background radiation. Generalized spectra efficiency models are used in PMT's and APD better understands of detection technologies. in PMT's we are using limiting envelope of the quantum efficiency of real-life PMT's with different types of photo cathodes.

Where in the APD's the spectral region is in between $1.0\mu m \le \lambda \le 1.1\mu m$

$$K_0 = \frac{\eta_{apd}.F_{pmt}}{\eta_{pmt}.F_{apd}} \qquad (4.6)$$

The quantum efficiency and K_0 parameter of both APD's and PMT's Vs. the wave length is shown in the **FIG 5.5**.

F.APD/PMT Signal to Noise Ratio Analysis

For weak lidar signals (0<P_S<1), in the absence of the background light, the PMT's signal/noise ratio is much higher than for the APD's for signal power values up to P_S=1. With increased background intensity, however, the photomultiplier noise dramatically increases and PMT loses its advantage over the APD[14,15].

$$K_p = SNR_{APD}/SNR_{PMT} \qquad (4.7)$$

Where, $SNR_{PMT} = \frac{\Psi_s^{PMT}}{\sqrt{\Psi_s^{PMT}+\Psi_b^{PMT}+Y_d^{PMT}}}$ in this $Y_d^{PMT} = I_d^{PMT}/I_q^{PMT}$

$SNR_{APD} = \frac{\Psi_s^{APD}}{\sqrt{\Psi_s^{APD}+\Psi_b^{APD}+Y_d^{APD}}}$ in this $Y_d^{APD} = I_d^{APD}/I_q^{APD}$

These are used to sketch the **FIG 5.6.**

G. Influence of Residual Skylight Background and Impact of "Noisy" APDs

Weak echo signal background superposition $\Psi_s+\Psi_b= (P_s+P_b)/P_q \ll 1$
Then,

$$K_p = K_o\sqrt{\frac{Y_d^{PMT}/Y_d^{APD}}{1+Y_{add}^{APD}}}=K_o\sqrt{x} \ll K_o (4.8)$$

Since as a rule $Y_d^{PMT}/Y_d^{APD} = I_d^{PMT}F_{APD}/I_d^{APD}F_{PMT} \ll 1$ and usually $0.1<Y_{add}^{APD}<10$
this equation for **FIG 5.7.**

H. Spectral dependences of the APD/PMT-SNR quotient at variations of normalized background power taking into account the additional noise of APD

Strong echo signal background superposition $\Psi_s+\Psi_b= (P_s+P_b)/P_q \gg 1$

Then, $K_p=K_o\sqrt{(P_s+P_b/P_q^{PMT})/(P_s+P_b/P_q^{APD})}$
$= \sqrt{K_o}(\lambda) \qquad (4.9)$
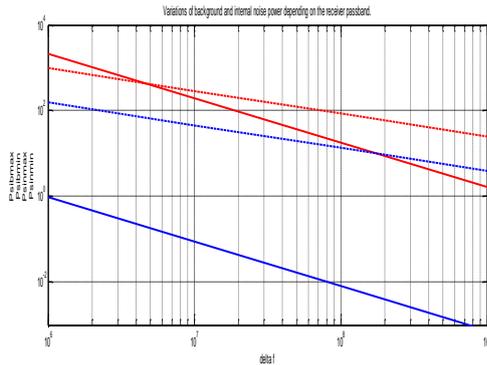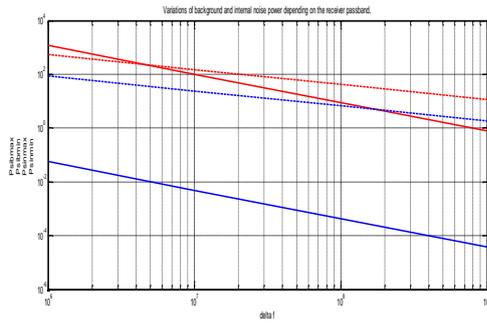
this is to implement **FIG 5.8**.

5. RESULTS

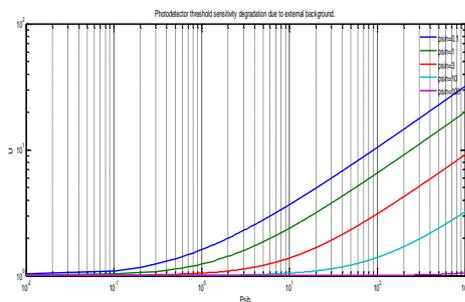Figure5.1: Variations Of Background And Internal Noise Depending On The Receiver pass band.

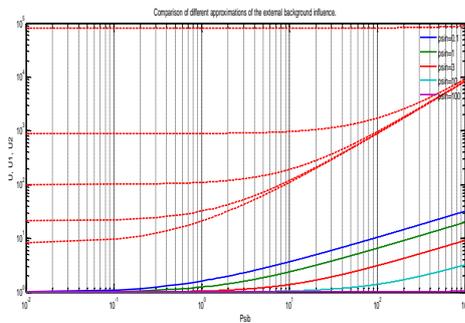Figure5.2: Photo Detector Threshold Sensitivity Degradation Due To External Background.

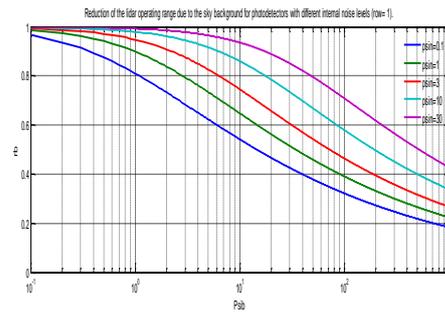Figure5.3: Comparison Of Different Approximations Of External Background Influence.

Figure5.4: Reduction Of Liadr Operating Range Due To Sky Background For Photo Detectors With Different Internal Noise Levels.
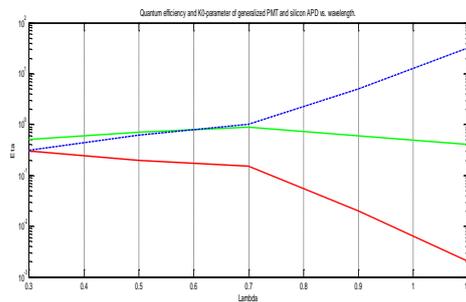

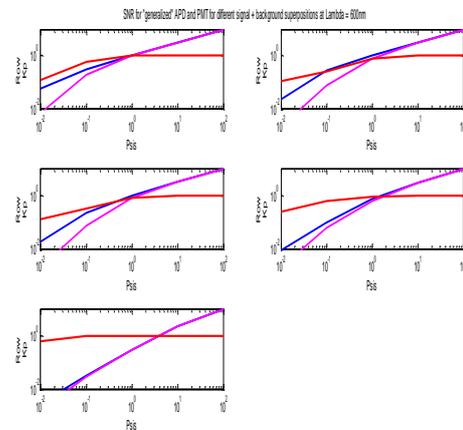Figure5.5: Quantum Efficiency Ko Parameter Generalized PMT And Silicon APD Vs Wave Length.

Figure 5.6: SNR for "Generalized" APD and PMT for different signal + background superpositions at lambda = 600nm.
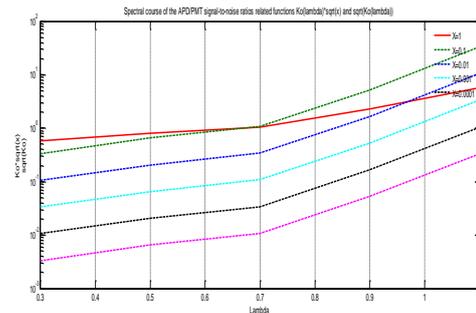

Figure5.7: Spectral Course Of APD/PMT Signal To Noise Ratios With Related Functions.
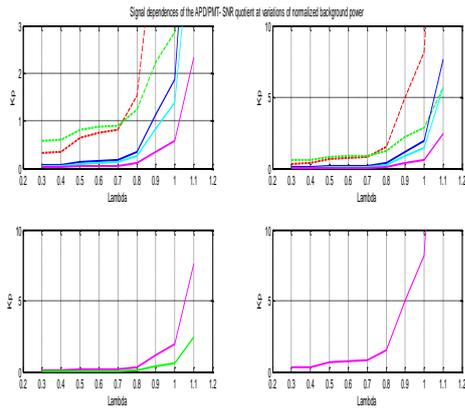
Figure5.8: Spectral Dependences Of APD/PMT SNR Quotient At Variations Of Normalized Background Power Tacking Into Account Additional Noise Of APD.

6. CONCLUSION

Matlab code has been implemented successfully for the estimation of signal to noise ratio between various detectors with different wavelengths. Also a good increment is seen between the APD and PMT from the comparison plots shown in all figures shown in this paper.

REFERENCES

[1] Hinkley E, editor. Laser monitoring of the atmosphere.Topics in Applied Physics, vol. 14. Berlin:Springler; 1978.

[2] Measures R. Laser remote sensing: fundamentals and applications. New York: Wiley; 1994.

[3] Bosenberg J, Brassington D, Simon P, editors. Instrument development foratmospheric research and monitoring: Lidar profiling, DOAS and TDLS. Berlin: Springer; 1997.

[4] Kovalev V, Eichinger W. Elastic lidar: theory, practice and analysis methods. New York: Wiley-Interscience;2004.

[5] Ross M. Laser receivers. New York: Wiley; 1966.

[6] Agishev R. Protection frombackgrounds in electro-optical systems of atmosphere monitoringMoscow: Mashinostroenie; 1994 [in Russian].

[7] Zuev V, Kaul B, Samokhvalov I. Laser sensing of industrial aerosol. Moscow: Nauka Press; 1996.

[8] Kopeika N. Background noise in optical communication systems. Proc. IEEE 1970;58(10):1365–84.

[9] Minkoff J. Signal processing fundamentals and applications for communications and sensing systems. Norwood: Artech House; 2002.

[10] Yakushenkov Yu, Lukantsev V, Kolosov M. Methods of struggle against clutter in electro-opticalsystems. Moscow: Radio i Svyaz; 1997 [in Russian].

[11] Agishev R, Comeron A. Spatial filtering efficiency of biaxial monostaticlidar: analysis andapplications. Appl Opt 2002;41(36):7516–21.

[12] Kingston R. Detection of optical and infrared radiation. Berlin: Springer; 1978.

[13] Arsenyev V, Davydov Yu. Receiving devices of optical range. Moscow: MAI-Press; 1992 [in Russian].

[14] Berkovskiy A, Gavanin V, Zaydel I. Vacuum photoelectronic devices. Moscow: Radio i Svyaz; 1998 [in Russian].

[15] Keiser G. Optical fibercommunication. NY: McGraw-Hill; 2000.

[16] Osche G. Optical detection theory for laser applications. New York: Wiley; 2002.